

Response to reviewer's comments - Reviewer 1

Authors: David Onnen, Gunner Chr. Larsen, Wai Hou Lio, Paul Hulsman, Martin Kühn, Vlaho Petrovic

Paper Number: WES-2024-188

Title: Field comparison of load-based wind turbine wake tracking with a scanning lidar reference

Color coding: Reviewer comments, authors responses, paper citations

Dear authors,

I enjoyed reviewing your well-written and relevant publication on the wake location estimator. One aspect I really value is the consideration of uncertainty and the resulting bounds. My criticism is mainly related to the methodology presentation. Some sections would benefit from some clarification and additional information.

Dear Reviewer,

First and foremost, thank you for taking the time to read through and review our manuscript. Answering your comments increased the quality of the manuscript. Thank you also for your positive words about the consideration of uncertainties and the writing of the manuscript. In the following we address each of your comments individually.

With kind regards,

The authors

Introduction

1) The introduction is, in my opinion, a bit too brief on related work and not formulated consistently. Please review the phrasing and connection of the different sentences to generate a better reading flow. In contrast, I think the discussion (section 4) is well written, especially the paragraph starting at Line 438, which connects this work well with similar ones.

The introduction section was revised, especially in regard to the phrasing. Further information on related work was added. The discussion section you highlighted is still the place, where the detailed comparison to other methodologies' results takes place. That allows the reader to compare and range the results of this work and the related works under consideration of the respective methodologies. In order to avoid double-mentioning, a reference to the discussion section was added in the introduction. The changes to the introduction section can be seen in the diff-document.

2) I am missing the motivation to use an extended Kalman Filter. Why not apply an Ensemble Kalman Filter or an Unscented Kalman Filter? The paragraph starting with line 36 lists several works that have done some sort of tracking, but I am missing a phrase more insight into how these publications have solved the issue, how the publications are connected, and what their successes and shortcomings are. I am also missing the link to the, in my opinion, relevant publications

Towards the multi-scale Kalman filtering of dynamic wake models: observing turbulent fluctuations and wake meandering, R. Braunbehrens et al 2023

and

Closed-loop coupling of a dynamic wake model with a wind inflow estimator, J. Di Cave et al 2024

The Extended Kalman Filter (EKF) was sufficient for this application - it is the simple-most and computationally most efficient form here. Note, that the dynamic model is already formulated as a linear system, thus only the measurement model needs a local linearization (this aspect is now added to section 2.2.1 explicitly). Reasons to use an Ensemble Kalman Filter (EnKF) or an Unscented Kalman Filter (UKF) would be a higher-dimensional problem or strong non-linearity of the model. Other authors works, e.g. (Becker et al., 2022) and (Braunbehrens et al., 2023) use wind farm models with a high number of observation points (>100). In these cases, the EnKF becomes more efficient than the local linearization with respect to each of the states.

Note, that the state transition model f used in this work can be formulated as a linear operation (see next subsection). Thus, the local linearisation in Equation 4 is not necessary in every iteration - F_k can be directly pre-computed.

The reference to (Braunbehrens et al., 2023) was added, both here and in 2.2.2 (regarding the distinction between time scales, together now with the work of (Rott et al., 2018; Simley et al., 2020)). The information contained in (J. Di Cave et al 2024) was considered covered by the works of Becker et al.

3) Line 24 - „encountered“ seems an odd choice. Do you mean „accounted for“?

Indeed, your suggestion sounds more suitable. It was implemented.

While robust formulations can account for wind direction variability (Rott et al., 2018; Simley et al., 2020), optimal wake deflection cannot be guaranteed, since outer influences and wake dynamics can hardly be accounted for.

4) Line 30 - Missing citation

Please excuse the inconvenience of this and thank you for pointing it out. It turned out to be a corrupted bibtex item that slipped our checks for the final compilation of the document. We have of course corrected this in the revised version for all occurrences of this reference (thus we will not address this aspect for the following instances individually in this authors response). The missing reference was (Kidambi Sekar et al., 2024).

Methodology

5) Line 78 - Wind shear exponent at 50Hz is used for what?

We apologize for the confusion. Of course, a wind shear exponent at 50 Hz is neither necessary nor sensible. “All so far mentioned measurements are stored at 50Hz” was said at this point, because the description of the lidar measurements with different sampling frequencies begins in the following. We changed the order of sentences to avoid any confusion.

[...] Both the turbine and met the mast data is stored at 50Hz.

The wind shear exponent α is calculated from the met mast measurements according to the power law: [...]

6) Line 98 - How does the height difference between the turbines affect this setup?

The height difference is accounted for in the generation of training data of the load-based estimator. The FASTfarm model uses the correct heights of the individual turbines. Assuming purely horizontal propagation of the wake, the lidar would probe the wake location at a slightly lower altitude than the hub height of WT2. Yet, the convolution method is not expected to be notably influenced regarding the lateral wake position it returns. Since only single PPI lidar scans are available, the exact vertical wake position cannot be addressed here. It is, however, also not in focus of wind farm flow control.

7) Line 109 - Is the assumption of zero mean justified? How are the matrices \mathbf{Q} and \mathbf{R} populated? Was some sort of normalization necessary?

Kalman filters by definition handle zero-mean white noise, thus the statement in Line 109 is to be seen as the plain definition of variables to be used within the filter. Since the wake dynamics are not modelled with white noise, the state augmentation is done as described in section 2.2.2, realizing the necessary noise shaping while maintaining the original Kalman filter equations. \mathbf{Q} and \mathbf{R} are diagonal matrices. Normalization needs to be considered for the dynamic model if the methodology is applied at a different sampling frequency. The state transition covariance of course rises, if a larger time increment is on hand. Further details on the noise tuning can be checked in (David Onnen et al., 2023) in an idealized environment and for a non-commercial turbine (thus not subject to confidentiality aspects regarding the loads).

8) Line 141-143 Please add a source or rephrase to make clear where this statement comes from.

This also refers to the DMW model by (Larsen et al., 2008), as described in the preceding two sentences. It is said now explicitly.

Wake meandering in the atmospheric boundary layer is driven by turbulence patterns considerably larger than the wake deficit scale (Trujillo et al., 2011). Larsen et al. (2008) introduced the DWM model, which translates this split of scales to a random walk trajectory, where the wake deficit is seen as a passive tracer. Larsen et al. define the default cut-off frequency of the meandering motion is defined as $f_c = u_\infty / (2D_w)$, where D_w is the wake diameter (in near wake applications also the rotor diameter D is a valid choice). Note, that this is the theoretical limit, up to which a wake deficit is regarded as a passive tracer. Lio et al. (2021) show in a field study with a lidar-based EKF featuring an auto-correlation term of the wake position time history that the dominant spectral share of the meandering motions can be up to a factor 10 slower.

9) Line 150 - The dynamic system for the wake center is, in principle, a random walk model. And, while a random walk's value is zero, an individual random walk is also expected to travel further away from the origin. Translated to the wake center, I would expect the model to be somewhat stable within a given region - if the wind direction does not change, we would expect the wake to meander within given bounds, e.g., $\pm 2D$. This is even more the case for the z component, where we expect the wake to be within a narrower corridor.

Can the equations easily be adapted to incorporate this behavior? One approach could be to adapt Eq. 8a) (and 8b), respectively) to $\dot{y}_w(t) = v_c(t) - k y_w(t) + n_{\{x,1\}}(t)$,

where k is a feedback constant. However, the change would cause the meandering around the origin, which can then be offset with a changing reference.

To be clear, I think the chosen approach is valid if the system is continuously corrected. I just wonder if you do see the same limitations of the model, or if I am missing something?

Thank you for sharing your thoughts and impulse on this topic! We agree with your statement “The dynamic system for the wake center is, in principle, a random walk model. And, while the expected value of the random walk is zero, an individual random walk can be expected to diverge from the origin.” The model formulation, however, is not considering an individual random walk. Instead, it describes the probability distribution of the wake dynamics via the additive process noise covariance. And a “self-correction” is achieved by the Kalman filter as you suggest, by including measurements at every iteration. Additionally, since the wind direction (and turbine yaw) can change to a constellation of ceasing wake impingement, it is in fact possible that the wake moves laterally “out of bounds” of WT2, such that it is not observable anymore.

The formulation with a reverting term that you suggest would formulate an Ornstein-Uhlenbeck (OU) process. This would be a valid choice indeed, for situations where the wake position meanders around zero or around a mean position. This would be the case in simulation environments or wind tunnel applications with a constrained wind direction. An OU process is in fact used in (D Onnen et al., 2024) to synthesize wake trajectories for artificial wake conditions in a wind tunnel. Note however, that the spectra of the OU process and a random walk is congruent, such that no implications on the observer formulation in this paper are on hand.

Including a mean-reverting term for the vertical wake position could be worth considering in future, to further improve the robustness of the estimation. The onset should however be checked in a test environment, where a vertical wake position reference is available.

10) Line 179 - What are typical values for „ b, c, d “? Do they have a major contribution or are they minor compared to the rest?

These are additional tuning parameters for the consistent description of the model equations. We cannot state the absolute values for the load offsets b and c here, but we can say that the onset is small in comparison to the wake-induced aerodynamic load imbalances. The parameter d , describing the yaw-tilt-coupling has a typical value of a few degrees ($<10^\circ$).

11) Line 181 - Can you elaborate on M_{\max} and R_{mix} ? What do they represent, and how do you determine them?

M_{\max} is the maximum amplitude of the yaw/tilt moment with respect to the wake position. This maximum is given when the wake is at distance $r_w = R_{\text{mix}}$, or in the 1D case $y_w = R_{\text{mix}}$. They are determined by fitting the parameter model to the training data. This explanation was added to the manuscript with the overview on the fitting parameters in Table 1 (see response to question 16).

12) Section 2.2.3 would strongly benefit from a figure to illustrate the different moments and angles, possibly also in connection with the incoming wake and the thereby resulting moments. The text is a bit tricky to follow the way it is written right now.

Thank you for this feedback. We now indicate the fitting parameters now in Figure 3 and Figure 4, which illustrate the parametric model (see response to question 16).

13) Section 2.2.3 should further emphasize the link between the states introduced in Section 2.2.2 and the output. Line 161 briefly mentions equation $h(x,n)$ but then doesn't mention it again.

We have restructured the section to make this link more conclusive now.

The measurement model h is a mapping from the state to the measurement - in this study a link from the wake centre position to the rotor loads. The model must fulfill certain criteria: It should be computationally inexpensive, such that it can be computed online in each filter iteration. Look-up tables with pre-computed information are preferable here, see e.g. (Schreiber et al., 2020; Soltani et al., 2013)). Moreover, the model has to be differentiable, such that its local sensitivity to a change in state or input can be determined. Finally, it should be robust and lead to a convergence of the estimate, even if the state at initialization is far off. The measurement vector y_k contains the Coleman transformed, non-rotating flapwise blade root bending moments according to Eq. 9. The time index k is omitted from the notation for better readability.

[...]

In the following, the parameterised model is derived in Equations 10-13. All fitting parameters introduced in this scope are listed in Table 1. The model is subsequently fitted to training data generated in aeroelastic simulations with enabled DWM model. Figure 3 shows the contour shape of the model and Figure 4 an example of training data and fitting.

[...]

14) Equation 9-12 are a bit confusing to me: (9) introduces a method to calculate M_{yaw} , M_{tilt} and M_{col} based on sensor data, (10) then discusses how to get $M^{\sim}(r_w)$, just to invert it to return a different way of also calculating M_{yaw} and M_{tilt} , followed by (12) which then tells the reader how to calculate $M^{\sim}(r_w)$. I think what you are missing is that the M_{yaw} and M_{tilt} from Eq(10) and (11) are estimates based on the estimate of $M^{\sim}(r_w)$, which is based on the estimated states. If this is the case, please adapt the notation with the (^) symbol and think about reversing the derivation: States $\rightarrow r_w$ and $\theta \rightarrow M^{\sim}(r_w) \rightarrow M_{yaw}$ and M_{tilt}
Maybe also add a similar block diagram to Fig. 2 with a more detailed flow of the signals.

By definition, the Kalman filter compares measurements y with the measurement estimates $\hat{y} = h(\hat{x}, u)$. It is, however, not common practise to use the (^) symbol within the formulation of the measurement model $h()$ (see e.g. (Brown & Hwang, 1992; Lio et al., 2021; Soltani et al., 2013)). We would like to keep the order of the derivation. But we added another clarification after Eq. 9, stating that the modelling starts here (see previous comment).

15) Line 214 - Review the grammar of the sentence

The sentence was adjusted.

For other cases, e.g. for larger streamwise spacing, a higher-dimensional LUT is required to adequately resolve the impact of turbulent mixing in the far-wake region.

16) Line 220 - I'd expect a list of the fitted parameters here / insight into the derived LuT.

Thanks for pointing this out. It was added.

Table 1. Fitting parameter for the measurement model $h()$

Parameter	Unit	Description
R_{mix}	m	wake overlap resulting in the largest yaw/tilt moment; an approximation is $R_{\text{mix}} = (R + R_w)/2$, i.e. the mean of rotor radius and wake deficit radius
\tilde{M}_{max}	Nm	maximal value of yaw/tilt moment (reached at wake overlap R_{mix})
b	Nm	wake-independent offset of yaw moment
c	Nm	wake-independent offset of tilt moment
d	°	phase angle to describe yaw-tilt-coupling
M_0	Nm	collective moment at full wake overlap
M_∞	Nm	collective moment at no wake overlap

17) Line 229 - I assume this is the azimuth of the lidar? Since the rotor azimuth was already defined with a variable in the previous sections. Maybe add a word to clarify that. Addition: Table 2 confirms that it's the Lidar azimuth; just change it here.

Yes, this is the lidar azimuth angle. It was adjusted as you suggest.

18) Equation 15 / 16 - Are γ_1 and γ_2 already defined?

Thanks for pointing this out. We added a definition prior to Table 2.

The nacelle yaw angles are denoted γ_1 and γ_2 for WT1 and WT2, respectively.

19) Section 2.3.1 would profit from a sketch showing the different coordinate systems in relation to each other. This also makes it easier to interpret the results later on.

We have added a sketch of the coordinate systems as you suggest.

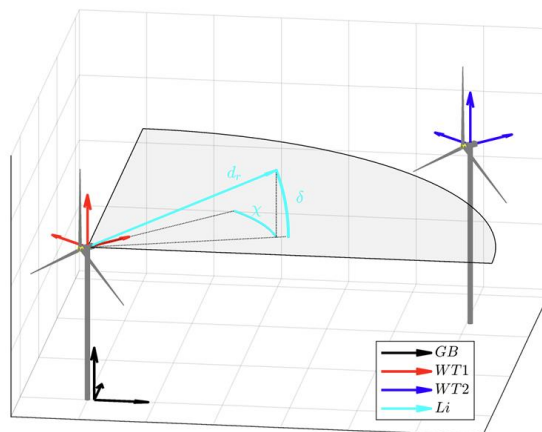


Figure 5. Illustration of the coordinate systems as defined in Table 2

20) Line 243 - Is this an issue in the comparison to the load-based approach? Both aim to determine the wake center but at different positions. This question is also related to the fact that the turbines seem to have different heights (as indicated in Section 2.1)

The impact on the comparison is assumed minimal. Assuming advection velocities of 5-10 m/s, the time difference between the upstream probing and the onset on the rotor is at the order of 10-20 seconds. Meanwhile, a lidar sample is recorded within 30s and the cut-off frequency of the wake dynamics for the EKF is 0.01 Hz. Thus, the impact of the different probing locations vanishes in comparison to the involved time scales of the wakes and their estimation.

It is true that we cannot compare at the exactly same positions, as it would be that case e.g. in an aeroelastic simulation with a DWM wind field that can be checked isolated for the wake position. We chose the best compromise by probing as close to the turbine as possible while also not being affected by the induction zone. This is the inaccessible reference in line 244, which investigates the induction zone in the same wind farm: (Kidambi Sekar et al., 2024). It describes how stream tube widening around the turbine leads to a lateral flow component, which redirects incoming partial wakes outwards.

Regarding the turbine height, please refer to our answer to comment 6.

21) Figure 5 has a very brief caption; I'd add where the data is coming from (lidar, I assume). Also, indicate the wind direction.

Thank you for pointing this out. The information on the data source (lidar indeed) and wind direction was added.

Figure 5. Wake centre identification from lidar measurements in WT2-based coordinate system. The wind direction here is 228° resulting in a full wake constellation.

22) Section 2.3.3 / Table 2 How are the uncertainties defined? Are the \pm values upper and lower bounds or standard deviations?

This is stated in the caption of Table 2 (now Table 3): "[...] values relate to the 95% confidence interval for normally distributed uncertainties". This means, that a coverage factor of 2 is used, so the $\pm 2\sigma$ bounds.

23) Figure 9 - Based on the explanation of „Geometry“ I would expect it to be a line / some sin or cos. However, around (205 deg, 150 m), the scattering shows a spread, the same for the other end of the data. How come?

That is really well spotted. The general expectation of the sine behaviour for the “Geometry” scatters is very well fulfilled. The small scattering you point out relates to instances of steep wind direction change, which is followed by a delayed yaw action of WT2. Since the wake position y_w is expressed in WT2-based coordinates, the deviation occurs. We consider no impact for the results of this paper.

24) Line 311 - There is no figure supporting the claim of the asymmetry during yawed conditions. Consider adding a second figure to Figure 11 with the data.

Thank you for bringing this up. Due to your comment, we have had another look at the binning with respect to yaw misalignment. It turned out that when applying high thresholds on the yaw misalignment ($>10^\circ$), a small trend is visible indeed: While the main asymmetry of the double Gaussian deficit, i.e. the magnitude difference of the two wake peaks, is still mainly linked to the ambient shear, we see a tendency towards a broader peak at the pronounced side of the wake at negative yaw misalignment. This finding is to be treated with care, since it is based on small data availability (compare Figure 9). We thus don't see enough evidence to make a generalized claim here, but the behaviour is in line with what we would expect according to literature on wakes of misaligned turbines (Bartl et al., 2018; Bromm et al., 2018; Sengers et al., 2020). The deviations we see could also explain for the slight RMSE increase of the tracking in case of negative yaw misalignments (see Figure 16), since the wake deficits slightly stand out from the others. We have done the following changes to include this to the paper:

- adding the plot to Figure 11 (now Figure 12) as you suggest
- describing the finding in section 3.1.2
- including the aspect to the discussion in section 4.1

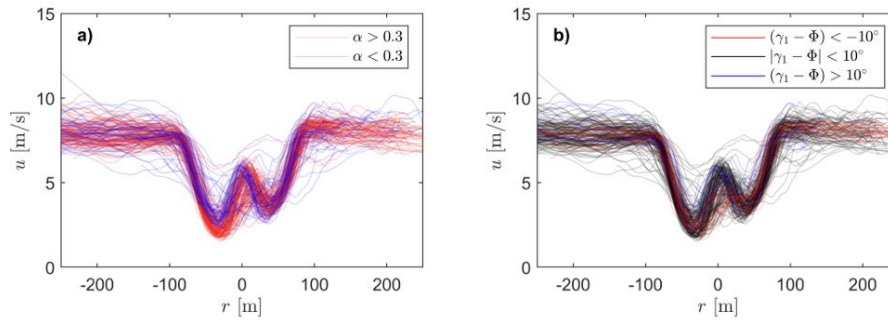


Figure 12. Wake deficits within wind speed bin $7.5 - 8 \text{ ms}^{-1}$; a) colour coded for two ranges of shear profile, defined by power law coefficient α ; b) colour coded with respect to yaw misalignment of WT1

In section 3.1.2

The co-occurrence of the asymmetry with ambient conditions is documented in Figure 12. A strong impact is visible when filtering for the power law coefficient α , describing the shear profile. Figure 12a indicates that the wake asymmetry is more pronounced at strong shear, connected to atmospheric stable conditions. For low shear coefficients, the wake deficits are rather symmetric. Larger wind speed variations among the deficits as well as in the non-waked area are on hand here, which again is attributed to the atmospheric stability. Figure 12b shows a distinction of wake deficits with respect to yaw-misalignment situations, which are known to cause a kidney-shaped curled wake (see e.g. Bartl et al., 2018; Sengers et al., 2023). While the main asymmetry of the double Gaussian deficit, i.e. the magnitude difference of the two wake peaks, is linked to the ambient shear, a tendency towards a broader peak at the pronounced side of the wake is seen in case of negative yaw misalignment. This finding is to be treated with care, since it is based on small data availability (compare Figure 9). The role of the wake deficit in this context is further discussed in section 4.1.

In section 4.1

The wake asymmetry is found to dominantly co-occur with strong wind shear and to increase with ambient wind speed, and thus also rotational speed. An interaction of wake rotation and the sheared flow is assumed. The rotational component in the wake flow, in opposite direction to the rotor rotation, could cause an 'upwash' of wind speeds from low altitudes on the right side of the rotor (facing downstream, thus negative on the y-axis) and a 'downwash' of wind speeds from higher altitudes on the left side. The direction of wake rotation and the observed orientation of the wake asymmetry would support this explanation. A comparable near wake asymmetry is reported by (Bromm et al., 2018) in a similar field campaign. A minor co-occurrence of wake asymmetry and large WT1 yaw misalignments ($>10^\circ$) is found, matching the expectation with regard to the curled wake phenomena (Bartl et al., 2018; Sengers et al., 2023). Yet, data availability of large yaw misalignments is not considered sufficient to draw a clear conclusion on curled wakes, which are also not in focus of this work.

25) Line 313 - I suggest to remove the „However“

The section was reformulated following the previous comment.

26) Figure 12 - The jet/rainbow colormap leads to severe misrepresentation of data and should not be used. For more information, see Figure 3 h) in *The misuse of colour in science communication*, Crameri et al. 2020, <https://www.nature.com/articles/s41467-020-19160-7>

Note that WES also cites this publication in their submission information <https://www.windenergy-science.net/submission.html#figurestable>

Thanks for addressing the topic and hinting at the reference. We have changed the colormaps of Figures 5,6,12 (now Fig. 6,7,13) accordingly. The recommended colormap 'viridis' is used.

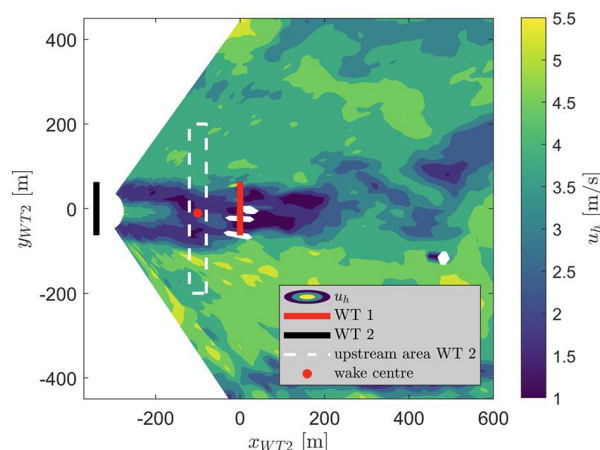


Figure 6. Wake centre identification from lidar measurements in WT2-based coordinate system. The wind direction here is 205° , resulting in a partial wake constellation.

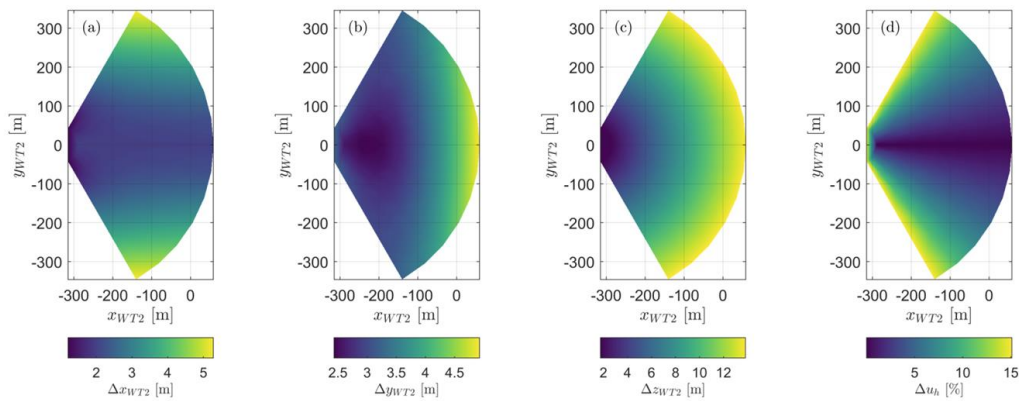


Figure 7. Illustration of uncertainty propagation: Probe position uncertainty in x, y, z and horizontal wind speed uncertainty; WT2-based coordinate system

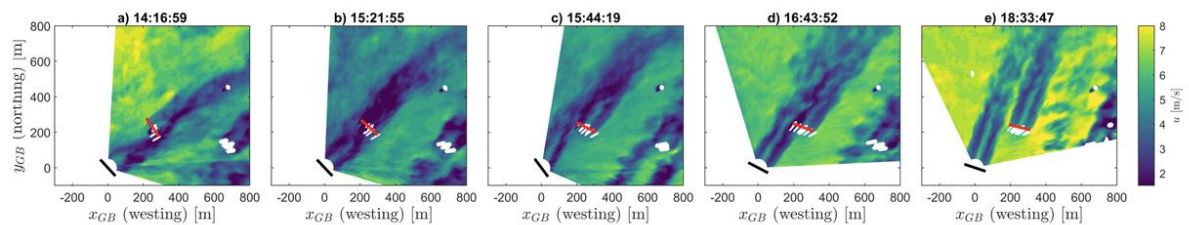


Figure 13. Top: Time series of wake position estimate by load-based EKF and lidar; the uncertainty range for both methods is indicated Bottom: Snapshots of the instantaneous flow situation in the wind farm; ground-based coordinates are used; WT1 indicated in black, WT2 in red; the time instances a-e refer to the indications in the time series plot on top

27) Figure 12 - a)-e) These are some of the main results of your paper, I'd increase the size of the figures significantly and add the then current wake location estimate. Consider removing double y-Axis for instance to get more space.

Thank you for pointing this out. The y-axis was removed for all but the leftmost snapshot, such that the figure size is increased. An example indication of the wake position estimate from lidar is given in Figure 6, which uses the WT2-based coordinate system. The visualisation in Figure 12 (now Figure 13) uses the ground-based coordinates for better overview of the general flow situation and turbine constellation.

28) Line 335 - Is it worth to add a subplot to Figure 12 with the yaw angle of WT1, and the wind direction? Additionally, Figure 12 does not indicate where the wake would be if it wasn't deflected due to the wake steering. If you add the geometric reference, this will become more visible.

Regarding the first aspect: The ambient conditions are shown in Figure 14, including the wind direction. The yaw misalignment of WT1 was added to the plot.

Regarding the second aspect: The geometric reference was intentionally not added in the top plot of Figure 12 (now Figure 13) for two reasons: i) as discussed in the context of Figure 10, the pure consideration of the farm geometry and the assumption of wake propagation parallel to the main wind direction is not capturing the wake position variability accurately. Also, occurrences of wake steering are just one aspect causing the wake position variability. ii) Adding another signal (plus its respective uncertainty range) would make the plot quite messy and distract from the main

comparison of this paper as mentioned in the title. Three overlapping uncertainty intervals with shading could hardly be told from one another.

29) Section 4.2 contains a lot of comparisons. Is it possible to visually put them next to each other? It might make it easier to see if there is a common trend or significant differences.

As elaborated, we consider a direct comparison of all approaches in literature not meaningful, since very different test scenarios and performance metrics are used. This is exactly the reason for this detailed section, addressing all approaches individually, under specific consideration of their respective setting and metric.

30) I am missing a Data & Code availability statement.

Thanks for pointing this out! The statement was added.

Bartl, J., Mühle, F., Schottler, J., Sætran, L., Peinke, J., Adaramola, M., & Hölling, M. (2018). Wind tunnel experiments on wind turbine wakes in yaw: Effects of inflow turbulence and shear. *Wind Energy Science*, 3(1), 329–343. <https://doi.org/10.5194/wes-3-329-2018>

Becker, M., Allaerts, D., & van Wingerden, J. W. (2022). Ensemble-Based Flow Field Estimation Using the Dynamic Wind Farm Model FLORIDyn. *Energies*, 15(22), 1–23. <https://doi.org/10.3390/en15228589>

Braunbehrens, R., Tamaro, S., & Bottasso, C. L. (2023). Towards the multi-scale Kalman filtering of dynamic wake models: observing turbulent fluctuations and wake meandering. *Journal of Physics: Conference Series*, 2505(1), 012044. <https://doi.org/10.1088/1742-6596/2505/1/012044>

Bromm, M., Rott, A., Beck, H., Vollmer, L., Steinfeld, G., & Kühn, M. (2018). Field investigation on the influence of yaw misalignment on the propagation of wind turbine wakes. *Wind Energy*, 21(11), 1011–1028. <https://doi.org/10.1002/we.2210>

Brown, R. G., & Hwang, P. Y. C. (1992). Introduction to random signals and applied kalman filtering (second edition), Robert Grover Brown and Patrick Y. C. Hwang, John Wiley, New York, 1992, 512 p.p., ISBN 0–47152–573–1, \$62.95. In *International Journal of Robust and Nonlinear Control* (Vol. 2, Issue 3). <https://doi.org/10.1002/rnc.4590020307>

Kidambi Sekar, A. P., Hulsman, P., Van Dooren, M. F., & Kühn, M. (2024). Synchronised WindScanner field measurements of the induction zone between two closely spaced wind turbines. *Wind Energy Science*, 9(7), 1483–1505. <https://doi.org/10.5194/wes-9-1483-2024>

Larsen, G. C., Madsen, H. A., Thomsen, K., & Larsen, T. J. (2008). Wake meandering: A pragmatic approach. *Wind Energy*, 11(4), 377–395. <https://doi.org/10.1002/we.267>

Lio, W. H., Larsen, G. C., & Thorsen, G. R. (2021). Dynamic wake tracking using a cost-effective LiDAR and Kalman filtering: Design, simulation and full-scale validation. *Renewable Energy*, 172, 1073–1086. <https://doi.org/10.1016/j.renene.2021.03.081>

Onnen, D, Neuhaus, L., Petrović, V., Ribnitzky, D., & Kühn, M. (2024). Dynamic wake conditions

tailored by an active grid in the wind tunnel. *Journal of Physics: Conference Series*, 2767(4), 042038. <https://doi.org/10.1088/1742-6596/2767/4/042038>

Onnen, David, Petrović, V., Neuhaus, L., Langidis, A., & Kühn, M. (2023). Wind tunnel testing of wake tracking methods using a model turbine and tailored inflow patterns resembling a meandering wake. *2023 American Control Conference (ACC)*, 837–842. <https://doi.org/10.23919/ACC55779.2023.10155916>

Rott, A., Doekemeijer, B., Seifert, J. K., van Wingerden, J.-W., & Kühn, M. (2018). Robust active wake control in consideration of wind direction variability and uncertainty. *Wind Energy Science*, 3(2), 869–882. <https://doi.org/10.5194/wes-3-869-2018>

Schreiber, J., Bottasso, C. L., & Bertelè, M. (2020). Field testing of a local wind inflow estimator and wake detector. *Wind Energy Science*, 5(3), 867–884. <https://doi.org/10.5194/wes-5-867-2020>

Sengers, B. A. M., Steinfeld, G., Heinemann, D., & Kühn, M. (2020). A new method to characterize the curled wake shape under yaw misalignment. *Journal of Physics: Conference Series*, 1618(6). <https://doi.org/10.1088/1742-6596/1618/6/062050>

Sengers, B. A. M., Steinfeld, G., Hulsman, P., & Kühn, M. (2023). Validation of an interpretable data-driven wake model using lidar measurements from a field wake steering experiment. *Wind Energy Science*, 8(5), 747–770. <https://doi.org/10.5194/wes-8-747-2023>

Simley, E., Fleming, P., & King, J. (2020). Design and analysis of a wake steering controller with wind direction variability. *Wind Energy Science*, 5(2), 451–468. <https://doi.org/10.5194/wes-5-451-2020>

Soltani, M. N., Knudsen, T., Svenstrup, M., Wisniewski, R., Brath, P., Ortega, R., & Johnson, K. (2013). Estimation of rotor effective wind speed: A comparison. *IEEE Transactions on Control Systems Technology*, 21(4), 1155–1167. <https://doi.org/10.1109/TCST.2013.2260751>

Trujillo, J.-J., Bingöl, F., Larsen, G. C., Mann, J., & Kühn, M. (2011). Light detection and ranging measurements of wake dynamics. Part II: two-dimensional scanning. *Wind Energy*, 14(1), 61–75. <https://doi.org/10.1002/we.402>